Journal of Colloid and Interface Science 343 (2010) 42–47

Contents lists available at ScienceDirect

Journal of Colloid and Interface Science

www.elsevier.com/locate/jcis

Stability analysis of an encapsulated microbubble against gas diffusion

Amit Katiyar, Kausik Sarkar *

Mechanical Engineering Department, University of Delaware, Newark, Delaware, USA

ARTICLE INFO

Article history:
Received 21 August 2009
Accepted 17 November 2009
Available online 20 November 2009

Keywords:
Epstein–Plesset
Contrast agent
Ultrasound imaging
Bubbles
Dissolution
Interfacial rheology
Stability

ABSTRACT

Linear stability analysis is performed for a mathematical model of diffusion of gases from an encapsulated microbubble. It is an Epstein–Plesset model modified to account for encapsulation elasticity and finite gas permeability. Although bubbles, containing gases other than air, are considered, the final stable bubble, if any, contains only air, and stability is achieved only when the surrounding medium is saturated or oversaturated with air. In absence of encapsulation elasticity, only a neutral stability is achieved for zero surface tension, the other solution being unstable. For an elastic encapsulation, different equilibrium solutions are obtained depending on the saturation level and whether the surface tension is smaller or higher than the elasticity. For an elastic encapsulation, elasticity can stabilize the bubble. However, imposing a non-negativity condition on the effective surface tension (consisting of reference surface tension and the elastic stress) leads to an equilibrium radius which is only neutrally stable. If the encapsulation can support a net compressive stress, it achieves actual stability. The linear stability results are consistent with our recent numerical findings. Physical mechanisms for the stability or instability of various equilibriums are provided.

© 2009 Elsevier Inc. All rights reserved.

1. Introduction

Bubbles appear in many natural and industrial situations due to sudden drop in ambient pressure. They critically affect a host of phenomena – from pumps to propellers [1–3], from air–sea exchange to sonar ranging, and from aeration to mixing [4]. Most recently bubbles have found biomedical applications as drug delivery [5,6] and contrast enhancing [7,8] agents. Free air bubbles of 1-μm radius last in a suspension for around 30 ms [9]. Surface tension generates a higher pressure inside the bubble which drives the gas to its eventual dissolution – it has been fully modeled in the classic article by Epstein and Plesset [10]. Therefore, sustained presence of very small bubbles is only possible in presence of an encapsulation which holds the gas in. In the ocean, the encapsulation is formed by naturally occurring organic substances. In man-made applications, surface active molecules are purposefully introduced for creating a stabilizing barrier at the interface. We have recently been investigating microbubble based ultrasound contrast agents [9,11–14]. These microbubbles are encapsulated by lipids (SonoVue, Definity, and Sonazoid), proteins (human serum albumin for Optison), and surfactants (SonoRx, Imavist). Although free bubble dynamics have been adequately modeled [10,15–18], there were very few models of bubble encapsulation [19,20].

Recently, we developed a rigorous mathematical model of an encapsulated microbubble incorporating explicitly the hindered gas permeability through encapsulation [9] and its elasticity [14]. We used it to numerically investigate the dynamics of contrast microbubbles. The model shows that encapsulation elasticity hinders bubble dissolution, and when it overcomes the surface tension, one obtains a stable microbubble. This explains the long shelf-life of commercial contrast microbubbles. We found that although the mathematical model predicts several equilibrium solutions, numerically only some of them are observed. In this paper, we explain this observation by performing a stability analysis of our model.

We briefly describe the mathematical model for the growth and dissolution of encapsulated microbubble, and report the governing set of ordinary differential equations for the linear stability analysis. We obtain the equilibrium bubble radius in a saturated and oversaturated medium, and determine the stability of these equilibrium solutions by a linear stability analysis. For the numerical calculations, we use the properties of FDA approved commercial contrast microbubble, Definity, which is an injectable lipid-encapsulated perfluoropropane microbubble.

2. Governing equations

We have previously described the model in detail [9,14]. Here we provide a brief sketch for completeness. Steady diffusion of gas is described by Laplace equation for the gas concentration C. The bubble contains gas at a concentration C_g. For the

* Corresponding author. Address: 126, Spencer Lab., Department of Mechanical Engineering, University of Delaware, Newark, DE 19716, USA. Fax: +1 302 831 3619.
E-mail address: sarkar@udel.edu (K. Sarkar).

0021-9797/$ - see front matter © 2009 Elsevier Inc. All rights reserved.
doi:10.1016/j.jcis.2009.11.030

encapsulation, we have developed an explicit model for gas permeation – a linear flux $h_g[C_w - C(R)]$, where h_g is the permeability through the encapsulation, and C_w is the gas concentration at the inside wall of the encapsulation. This in turn is related with C_g by Ostwald coefficient $C_w = L_g C_g$. Permeability h_g embodies the interaction between the gas molecules and the molecules of the encapsulation. It might be thought to result from either a Fickian diffusion ($h_g \approx k_g^e/\delta$, k_g^e is the diffusivity of the gas through the encapsulation and δ the thickness of encapsulation) or an energy barrier that a gas molecule has to overcome, the latter being possibly more appropriate for a monolayer [9,19,21,22]. The flux through the encapsulation is matched by the diffusive flux in the liquid at $r = R$.

$$-k_g \left.\frac{\partial C}{\partial r}\right|_R = h_g[L_g C_g - C(R)], \tag{1}$$

where k_g is the diffusivity in the surrounding liquid. One obtains a monopole solution for the Laplace equation:

$$C(r) = \frac{R^2(L_g C_g - C(\infty))}{r\left(\frac{k_g}{h_g} + R\right)} + C(\infty). \tag{2}$$

The mass conservation relates the radius change with the surface flux at $r = R$ to obtain

$$\frac{d}{dt}\left(\frac{4}{3}\pi R^3 C_g\right) = 4\pi R^2 k_g \left.\frac{\partial C}{\partial r}\right|_R = -4\pi R^2 k_g \frac{(L_g C_g - C(\infty))}{\left(\frac{k_g}{h_g} + R\right)}. \tag{3}$$

For a bubble containing air ($g = A$), we obtain

$$\frac{d(R^3 C_A)}{dt} = 3R k_A L_A \frac{\left(f\frac{p_{\text{atm}}}{R_G T} - C_A\right)}{\left(\frac{k_A}{h_A R} + 1\right)}. \tag{4}$$

We use $C_A(\infty) = f L_A p_{\text{atm}}/R_G T$, with f deciding whether the liquid is saturated ($f = 1$), undersaturated ($f < 1$) or oversaturated ($f > 1$) with air at the atmospheric pressure p_{atm}. R_G is the universal gas constant.

The pressure inside the bubble is larger than the outside atmospheric pressure by the Laplace pressure:

$$p_g = p_A = C_A R_G T = p_{\text{atm}} + \frac{2\gamma(R)}{R}. \tag{5}$$

For a Newtonian interfacial rheology, surface tension is constant, $\gamma(R) = \gamma_0$ as was the case considered by Epstein and Plesset [10]. For an elastic encapsulation, the encapsulation develops a stress on its surface as a result of fractional change in its area. It is equivalent to introducing a varying surface tension with surface elasticity $E^s = d\gamma/(dA/A_0)$:

$$\gamma(R) = \begin{cases} \gamma_0 + E^s\left[\left(\frac{R}{R_0}\right)^2 - 1\right], & \text{for } \gamma_0 + E^s\left[\left(\frac{R}{R_0}\right)^2 - 1\right] > 0, \\ 0, & \text{for } \gamma_0 + E^s\left[\left(\frac{R}{R_0}\right)^2 - 1\right] \leqslant 0. \end{cases} \tag{6}$$

where we have imposed a restriction $\gamma(R) \geqslant 0$. Note that we assume the initial radius $R(t = 0) = R_0$ to be the stress-free state. The second term in the first condition of (6) is an elasticity term, in that it gives rise to a compressive interfacial stress for $R < R_0$ and a tensile one for $R > R_0$. Note that, one might choose not to enforce non-negativity on the effective surface tension $\gamma(R)$ – the surface tension γ_0 and interfacial elasticity E^s can be introduced independently as material parameters. In that case, the first expression in (6) will suffice to describe the effective interfacial stress for the entire range. The non-negativity condition explicitly imposed in the second part of Eq. (6) prevents development of a net compressive stress on the encapsulation. A compressive stress would induce Euler buckling type behavior of the encapsulation. In reality, the encapsulating membrane would be endowed with a non-zero bending modulus which would govern the bending behavior. However, for the present purpose where a spherical symmetry is imposed, the model effectively assumes that the bending rigidity is sufficient to avoid buckling [23].

We non-dimensionalize various variables:

$$\widehat{\gamma}_0 = \frac{2\gamma_0}{p_{\text{atm}} R_0}, \quad \widehat{E^s} = \frac{2E^s}{p_{\text{atm}} R_0}, \quad \widehat{R} = \frac{R}{R_0}, \quad \alpha_A = \frac{k_A}{h_A R_0},$$

$$A = \widehat{R}^3 \frac{C_A R_G T}{P_{\text{atm}}}, \quad \tau = \frac{k_F}{R_0^2} t, \quad \widehat{\gamma} = \widehat{\gamma}_0 + \widehat{E^s}(\widehat{R}^2 - 1),$$

and obtain for Eqs. (4) and (5):

$$\frac{dA}{d\tau} = \frac{-3\beta L_A (A - f\widehat{R}^3)}{\widehat{R}(\alpha_A + \widehat{R})}, \tag{7}$$

$$A = \begin{cases} \widehat{R}^3 + \widehat{\gamma}_0 \widehat{R}^2 + \widehat{E^s}\widehat{R}^2(\widehat{R}^2 - 1), & \text{for } \widehat{\gamma} > 0, \\ \widehat{R}^3, & \text{for } \widehat{\gamma} = 0. \end{cases} \tag{8}$$

One can differentiate (8) and using (7) and (8), we obtain an equation for $\widehat{R}(\tau)$:

$$\frac{d\widehat{R}}{d\tau} = \begin{cases} \frac{-3L_A\left[\widehat{R}(1-f) + \widehat{\gamma}_0 + \widehat{E^s}(\widehat{R}^2 - 1)\right]}{(\alpha_A + \widehat{R})\left(3\widehat{R}^3 + 2\widehat{\gamma}_0\widehat{R}^2 + 2\widehat{E^s}\widehat{R}^4\right)}, & \text{for } \widehat{\gamma} > 0, \\ \frac{-L_A(1-f)}{(\alpha_A + \widehat{R})}, & \text{for } \widehat{\gamma} = 0. \end{cases} \tag{9}$$

The inelastic case (Newtonian interfacial rheology with constant surface tension) can be obtained for $\widehat{E^s} = 0$. Note that undersaturation ($f < 1$) and positive effective surface tension ($\widehat{\gamma}_0 + \widehat{E^s}(\widehat{R}^2 - 1) > 0$) make $d\widehat{R}/dt$ negative, leading to bubble dissolution. Undersaturation allows more gas to go into solution. On the other hand $f > 1$ leads to an opposite effect favoring gas flow into the bubble from the liquid tending to increase the bubble size.

3. Equilibrium solutions and their stability

For a set of ordinary differential equations (ODE),

$$\frac{d\mathbf{x}}{dt} = \mathbf{G}(\mathbf{x}), \tag{10}$$

with equilibrium solution $\mathbf{x}_{eqb}$ ($\mathbf{G}(\mathbf{x}_{eqb}) = 0$), the stability is determined by the eigenvalues λ_k's of the Jacobian $\mathbf{J}|_{\mathbf{x}_{eqb}} = \partial\mathbf{G}/\partial\mathbf{x}|_{\mathbf{x}_{eqb}}$, in that a small perturbation $\delta\mathbf{x}$ evolves as $\delta\mathbf{x} \sim \sum_k \psi_k \mathbf{x}_k e^{\lambda_k t}$ (ψ_k's are scalars). $\mathbf{x}_k$'s are the corresponding eigenvectors. If the real part of all eigenvalues is negative, equilibrium solution $\mathbf{x}_{eqb}$ is stable, and otherwise it is unstable. For a single ODE as in Eq. (9) stability of equilibrium solution (x_{eqb}) requires $\partial G/\partial x|_{x_{eqb}}$ to be negative. We obtain the equilibrium solution for the bubble radius from (9) by equating the left hand side to zero. We find two equilibriums for inelastic interface ($\widehat{E^s} = 0$), and four other for elastic interface, to be studied below.

3.1. Inelastic cases

Solution 1: For zero interfacial tension ($\widehat{\gamma}_0 = 0$) and saturated medium ($f = 1$), $\frac{d\widehat{R}}{d\tau}$ is zero for any bubble radius. It relates to $p_g = p_A = p_{\text{atm}}$. Therefore it is a neutral equilibrium, as was seen by our numerical exploration [9]; one obtains a long time stable bubble equilibrium which depends on the initial bubble radius. The pressure equilibrium being independent of the radius indicates

that changing radius does not affect the stability which explains the neutral stability of the equilibrium.

Solution 2:

$$\widehat{R}_{eqb} = \frac{\widehat{\gamma}_0}{(f-1)} \quad \text{for } f > 1 \tag{11}$$

It is unstable as

$$\left.\frac{\partial G}{\partial \widehat{R}}\right|_{R_{eqb}} = \frac{3L_A(f-1)}{(\alpha_A + \widehat{R}_{eqb})(3\widehat{R}_{eqb} + 2\widehat{\gamma}_0)} > 0. \tag{12}$$

Indeed, we found unconstrained bubble growth for an oversaturated case in Ref. [9]. One can understand the unstable nature of the equilibrium by examining the Eq. (5) with a constant surface tension $\gamma = \gamma_0$. If the radius is increased by a small amount from its equilibrium value, the surface tension term $2\gamma_0/R$ becomes smaller. Therefore, the inside pressure and thereby the inside gas concentration is decreased facilitating diffusion of gas into the bubble which further increases the bubble radius. On the other hand, if the radius is decreased by a small amount from the equilibrium, the concentration inside increases leading to an outward diffusion of gas from the bubble and causes further shrinking. The phenomenon is explained in Fig. 1a.

3.2. Elastic cases

Solution 3:

$$\widehat{R}_{eqb} = \sqrt{\left(1 - \frac{\widehat{\gamma}_0}{\widehat{E}^s}\right)} \quad \text{for } f = 1 \quad \text{and } \widehat{E}^s > \widehat{\gamma}_0, \tag{13}$$

This equilibrium solution corresponds to effective surface tension (6) being zero. The equilibrium radius R_{eqb} is less than the stress-free radius R_0 which results in an elastic compressive stress that balances the tensile stress due to γ_0. When the non-negativity is introduced on surface tension in (6), the discontinuous surface tension makes $\partial G/\partial x|_{x_{eqb}}$ at the equilibrium point discontinuous. We determine it from both sides of the discontinuity:

$$\left.\frac{\partial G}{\partial \widehat{R}}\right|_{R^+_{eqb}} = \frac{-6L_A\widehat{E}^s\widehat{R}_{eqb}}{(\alpha_A + \widehat{R}_{eqb})\left[3\widehat{R}_{eqb} + 2\left(\widehat{E}^s - \widehat{\gamma}_0\right)\right]} < 0, \tag{14}$$

$$\left.\frac{\partial G}{\partial \widehat{R}}\right|_{R^-_{eqb}} = 0. \tag{15}$$

Therefore, for cases where surface tension is not forced to be negative, relation (14) is applicable from both above and below R_{eqb}, making it a stable equilibrium. For surface tension given with two different expressions (6), the equilibrium point is stable as the bubble size is diminishing. However, after the bubble reaches zero surface tension, it reverts to solution 1 upon further decrease of bubble radius, i.e. it reaches neutral stability. As has been noted above, the non-negativity condition is not essential. The encapsulation, when it reaches a maximum packing can sustain compressive stress upon further decrease in radius. It is also interesting to note that in view of the above, imposing non-negativity on surface tension does not lead to a stable radius in an air-saturated medium. However, allowing the encapsulation to sustain net compressive stress makes the equilibrium radius stable. The stability can be understood by again investigating pressure equilibrium (5) under the condition of a slightly deformed bubble (also shown in Fig. 1b). If the bubble radius is increased from equilibrium, the elastic stress would increase the effective surface tension $\gamma(R)$. The term $2\gamma(R)/R$ would increase as the decreasing effect from the denominator is of a higher order in the small change in radius. Therefore, unlike the solution 2, here it would increase inside pressure and concentration leading to expulsion of gas which brings the radius back to the equilibrium. Similarly, when non-negativity is not imposed (surface tension is given by only the first condition in (6)), decreasing the bubble radius slightly from the equilibrium would decrease $2\gamma(R)/R$, which results in an decreased inside pressure and concentration leading to gas influx bringing again the radius back to equilibrium.

Solution 4:

$$\widehat{R}_{eqb} = \varepsilon + \sqrt{\varepsilon^2 + \left(1 - \frac{\widehat{\gamma}_0}{\widehat{E}^s}\right)} \quad \text{for } f > 1 \quad \text{and } \widehat{E}^s > \widehat{\gamma}_0,$$
$$\text{where } \varepsilon = \frac{(f-1)}{2\widehat{E}^s} \tag{16}$$

$$\left.\frac{\partial G}{\partial \widehat{R}}\right|_{R_{eqb}} = \frac{-6L_A\widehat{E}^s(\widehat{R}_{eqb} - \varepsilon)}{(\alpha_A + \widehat{R}_{eqb})\left[3\widehat{R}^3_{eqb} + 2\widehat{\gamma}\,\widehat{R}^2_{eqb} + 2\widehat{E}^s\widehat{R}^4_{eqb}\right]} < 0 \quad \text{as } \widehat{R}_{eqb} > \varepsilon$$
$$\text{and } \widehat{\gamma} > 0.$$

And therefore the equilibrium is stable for this oversaturated case. Indeed, we obtained this solution numerically [14]. Note that in this case, both of the conditions $\widehat{E}^s > \widehat{\gamma}_0$ (making the solution 3 stable) and oversaturation $f > 1$ are stabilizing, and therefore stability is expected. The reasoning is similar to the one given for solution 3.

Solutions 5 and 6: With $f > 1$, but $\widehat{E}^s < \widehat{\gamma}_0$ and $\varepsilon^2 \geqslant \left(1 - \frac{\widehat{\gamma}_0}{\widehat{E}^s}\right)$, $\varepsilon = \frac{(f-1)}{2\widehat{E}^s}$,

$$\widehat{R}_{eqb_1} = \varepsilon + \sqrt{\varepsilon^2 + \left(1 - \frac{\widehat{\gamma}_0}{\widehat{E}^s}\right)}, \tag{17}$$

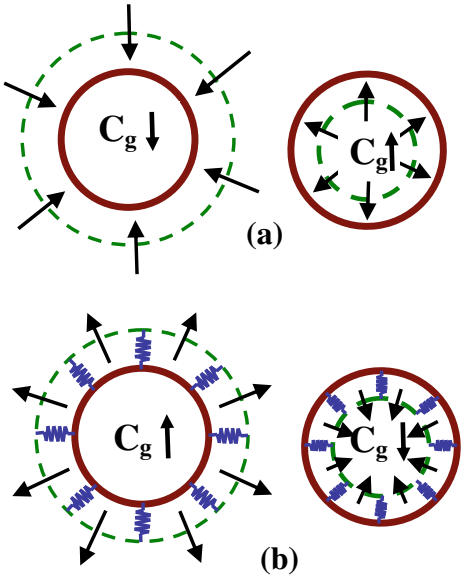

Fig. 1. Mechanisms for unstable equilibrium for an inelastic encapsulation (a) and stable equilibrium for an elastic encapsulation (b). In (a) increasing or decreasing radius (green dashed line) from the equilibrium (brown solid line) leads to gas movement (radial arrows) to further drive it away from the equilibrium. Corresponding increase or decrease of inside gas concentration C_g causes the gas flux. Opposite happens in (b). (For interpretation of the references to colour in this figure legend, the reader is referred to the web version of this article.)

$$\widehat{R}_{eqb_2} = \varepsilon - \sqrt{\varepsilon^2 + \left(1 - \frac{\widehat{\gamma}_0}{\widehat{E}^s}\right)}, \tag{18}$$

$$\frac{\partial G}{\partial \widehat{R}} = \frac{-6L_A\widehat{E}^s(\widehat{R}-\varepsilon)}{(\alpha_A+\widehat{R})\left[3\widehat{R}+2(\widehat{\gamma}_0-\widehat{E}^s)+4\widehat{E}^s\widehat{R}^2\right]} \begin{cases} <0, & \text{for } \widehat{R}^1_{eqb}, \\ >0, & \text{for } \widehat{R}^2_{eqb}. \end{cases}$$

Therefore, only one equilibrium solution $\widehat{R}^1_{eqb}$ is stable and it is the one numerically seen in the oversaturated case with $\widehat{\gamma}_0 > \widehat{E}^s$ [14].

4. Effects of multiple gases

To ensure long shelf-life, second generation contrast microbubbles are filled with perfluorocarbon gas (also known as osmotic agent) due to its lower diffusivity and solubility compared to air. Upon introduction in blood or water, dissolved air diffuses into the bubble and makes the bubble a multi-component system – air (A) and an osmotic agent (F). We obtain following conservation equation for F from (3):

$$\frac{d(R^3C_F)}{dt} = -3Rk_F\frac{L_FC_F}{\left(\frac{k_F}{h_FR}+1\right)}, \tag{19}$$

where we use $C_F(\infty) = 0$. Using non-dimensional variables.

$$F = \widehat{R}^3\frac{C_FR_GT}{p_{\text{atm}}}, \quad \beta = \frac{k_A}{k_F} \quad \text{and } \alpha_F = \frac{k_F}{h_FR_0},$$

the non-dimensional form of (19) and (4) reduces to:

$$\frac{dF}{d\tau} = \frac{-3L_FF}{\widehat{R}(\alpha_F+\widehat{R})}, \tag{20}$$

$$\frac{dA}{d\tau} = \frac{-3\beta L_A(A-f\widehat{R}^3)}{\widehat{R}(\alpha_A+\widehat{R})}. \tag{21}$$

The pressure balance equation at the gas liquid interface of the bubble becomes:

$$p_g = p_A + p_F = (C_A+C_F)R_GT = p_{\text{atm}} + \frac{2\gamma(R)}{R}, \tag{22}$$

which upon non-dimensionalization gives:

$$A+F = \begin{cases} \widehat{R}^3 + \widehat{\gamma}\,\widehat{R}^2, & \text{for } \widehat{\gamma} > 0 \\ \widehat{R}^3, & \text{for } \widehat{\gamma} = 0 \end{cases}, \tag{23}$$

using surface tension expression (6). Differentiating (23) and using (21) and (20), we replace the equation of F by

$$\frac{d\widehat{R}}{d\tau} = \begin{cases} \frac{-3}{(3\widehat{R}^3+2\widehat{\gamma}\,\widehat{R}^2+2\widehat{E}^s\widehat{R}^4)}\left[\frac{\beta L_A(A-f\widehat{R}^3)}{(\alpha_A+\widehat{R})}+\frac{L_F\{\widehat{R}^3+\widehat{\gamma}\,\widehat{R}^2-A\}}{(\alpha_F+\widehat{R})}\right], & \text{for } \gamma > 0, \\ \frac{-3}{(3\widehat{R}^3+2\widehat{E}^s\widehat{R}^4)}\left[\frac{\beta L_A(A-f\widehat{R}^3)}{(\alpha_A+\widehat{R})}+\frac{L_F\{\widehat{R}^3-A\}}{(\alpha_F+\widehat{R})}\right], & \text{for } \gamma = 0. \end{cases} \tag{24}$$

From (20), we note that at equilibrium, perfluorocarbon completely diffuses out of the bubble ($F = 0$) and two-gas pressure balance (23) reduces to the single-gas balance (8). The conservation Eq. (21) for A gives the equilibrium solution for A

$$A_{eqb} = f\widehat{R}^3_{eqb},$$

and using it in (23) then shows that the equilibrium solutions for the two-gas case are the same as those for a single gas (air) as in Section 3 (Eqs. (11)–(18)). However, the stability of these equilibrium solutions might get affected by the introduction of a second gas. Next, we investigate the two-gas case, governed by Eqs. (21) and (24), from which we compute the Jacobian and its eigenvalues. The expression for the Jacobian is provided in Appendix A. Unlike for air bubbles, the algebra here is complicated and therefore analytical expressions for eigenvalues are provided only for the case (solution 1) of an inelastic encapsulation in a saturated medium. For all other cases, eigenvalues are computed numerically using property values representative of the Definity contrast microbubble, which was also the case treated in our previous articles [13,14]. The property values for Definity are listed here in Table 1. However, we also study the effects of variation in the property values.

Table 1
Physical properties used in simulations.

Initial bubble radius (R_0)	1.25×10^{-6} (m)
Atmospheric pressure (p_{atm})	101325 Pa
Coefficient of diffusivity of air in water (k_A)	2.05×10^{-9} m^2 s^{-1}
Coefficient of diffusivity of C_3F_8 in water (k_F)	7.45×10^{-10} m^2 s^{-1}
Surface tension (γ_0)	0.025 N/m
Ostwald coefficient of C_3F_8 (L_F)	5.2×10^{-4}
Ostwald coefficient of air (L_A)	1.71×10^{-2}
Permeability of air through the encapsulation (h_A)	2.857×10^{-5} m s^{-1}
Permeability of C_3F_8 through the encapsulation (h_F)	1.2×10^{-6} m s^{-1}

Solution 1: In this inelastic saturated ($f = 1$) case, we find

$$\underline{\underline{J}}|_{R_{eqb}A_{eqb}} = \begin{bmatrix} \frac{3\{\beta L_A(\alpha_F+\widehat{R}_{eqb})-L_F(\alpha_A+\widehat{R}_{eqb})\}}{\widehat{R}(\alpha_F+\widehat{R}_{eqb})(\alpha_A+\widehat{R}_{eqb})} & \frac{-\{\beta L_A(\alpha_F+\widehat{R}_{eqb})-L_F(\alpha_A+\widehat{R}_{eqb})\}}{\widehat{R}^3_{eqb}(\alpha_F+\widehat{R}_{eqb})(\alpha_A+\widehat{R}_{eqb})} \\ \frac{9\beta L_A\widehat{R}_{eqb}}{(\alpha_A+\widehat{R}_{eqb})} & \frac{-3\beta L_A}{\widehat{R}(\alpha_A+\widehat{R}_{eqb})} \end{bmatrix} \tag{25}$$

Eigenvalues:

$$\lambda_1 = 0 \text{ and } \lambda_2 = -\frac{3L_F}{\widehat{R}_{eqb}(\alpha_F+\widehat{R}_{eqb})}$$

The equilibrium solution corresponds to $A_{eqb} = \widehat{R}^3_{eqb}$ and $p_g = p_A = p_{\text{atm}}$. Note that for the corresponding case for an air bubble, we find a zero growth rate, which corresponds to the zero eigenvalue here. Indeed the result was found in our numerical study in [9] (note that the corresponding Fig. 8 in [9] has the surface tension labels erroneously reversed).

Solution 2: For this oversaturated ($f > 1$) case and the cases below, we use the Definity properties (Table 1). We find the eigenvalues to be $\lambda_1 = 1.522 \times 10^{-4}$ and $\lambda_2 = -3.2 \times 10^{-6}$, therefore rendering it unstable; introduction of the second gas does not change stability of the equilibrium solution, as was also seen in numerical solution [14]. In Figs. 2 and 3, we find that changing the property values of the second gas such as permeability (non-dimensionalized as α_F) and Ostwald coefficient L_F does not change the positive eigenvalues λ_1, but affects the other one. One can then conclude that the positive eigenvalue is dominated by the air properties, which in the single gas case, we see, also leads to a positive growth rate. On the other hand, in Fig. 4, changing air permeability h_A affects the positive eigenvalue, but leaves the other unaltered. Changing initial radius (Fig. 5) changes both eigenvalues, however once again preserving the overall instability of the equilibrium. We also note in Fig. 2 that the negative eigenvalue λ_2 approaches zero for very high α_F, i.e. for very low permeability, the gas cannot go in or out of the bubble and therefore, does not affect the dynamics. Similarly in Fig. 3, for very low solubility of the second gas, we find $\lambda_2 \to 0$.

Solution 3: For this equilibrium solution in a saturated medium, we note that the Jacobian (Eqs. (14) and (15)) is discontinuous because of the non-negative condition on the surface tension. For the

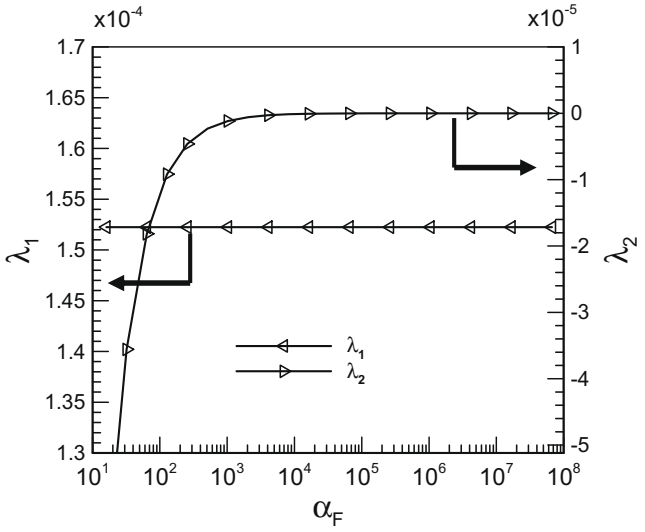

Fig. 2. Variation of eigenvalues with α_F for a perfluorocarbon bubble for solution 2.

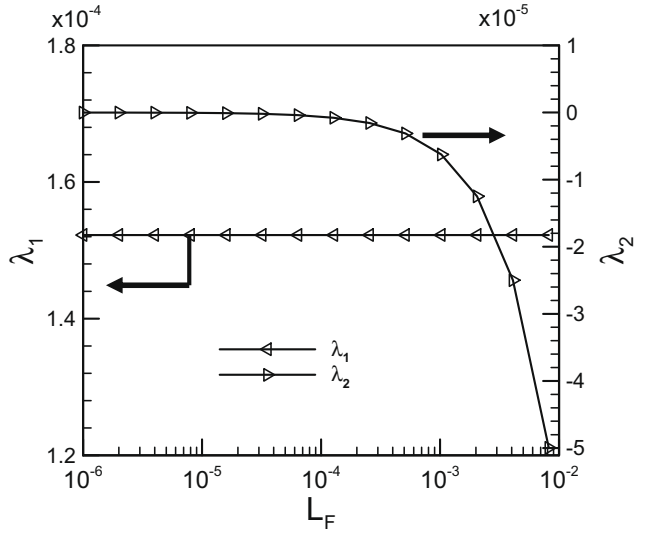

Fig. 3. Variation of eigenvalues with L_F for a perfluorocarbon bubble for solution 2.

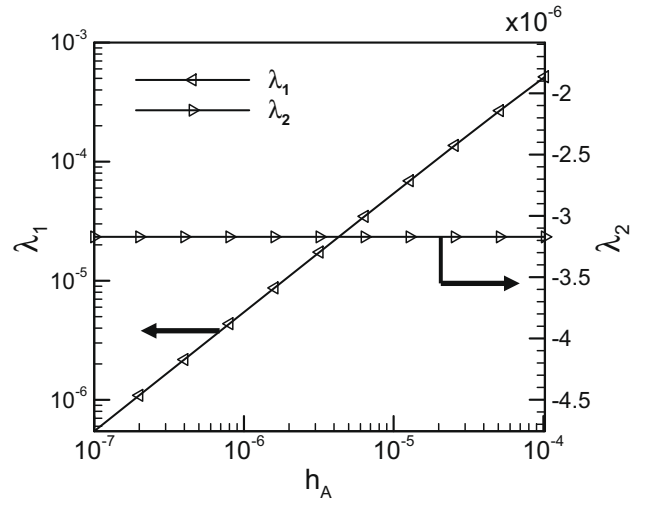

Fig. 4. Variation of eigenvalues with h_A for a perfluorocarbon bubble for solution 2.

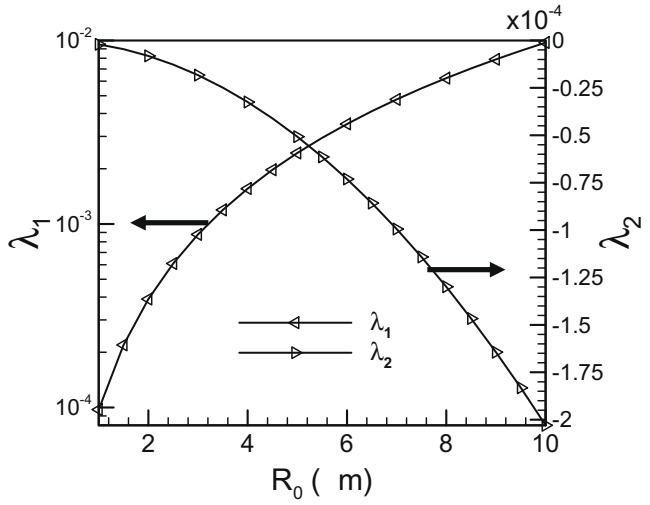

Fig. 5. Variation of eigenvalues with R_0 for a perfluorocarbon bubble for solution 2.

two-gas case, the same condition persists. With $E^s = 0.04$ N/m, we find

$$\widehat{R}_{eqb} = 0.6124,\ A_{eqb} = 0.2296;$$

$$\lambda_1^+ = -5.1 \times 10^{-6} \text{ and } \lambda_2^+ = -8.145 \times 10^{-4}$$

$$\lambda_1^- = 0 \text{ and } \lambda_2^- = -1.9 \times 10^{-3}$$

Similar to the single gas case, if the non-negative condition is not imposed, the same expression of surface tension holds above and below the equilibrium point and therefore, eigenvalues (indicated by the + superscript) being real and negative indicate linear stability for this solution. Therefore, in this saturated liquid, one obtains a stable microbubble. However, when the dual expressions (6) for surface tension are imposed, one obtains stability only for positive perturbations, and for negative perturbations the solution is again neutrally stable. Effects of variation in properties are similar to solution 2, and are not shown here.

Solution 4, 5 and 6: Table 2 reports the results for these equilibriums in oversaturated media. The specific values of saturation levels and interfacial elasticity are also provided. We note that the solution 4 corresponds to stabilizing influence of interfacial elasticity compensating for destabilizing surface tension and is shown to be stable for the single gas case. It remains stable with both eigenvalues negative for the two-gas case. For surface tension more than elasticity (we choose 0.01 N/m for the latter, see Table 2), oversaturation is the stabilizing influence. It gives rise to two solutions 5 and 6. As with the single gas case, the solution 5 is stable, and the solution 6 is unstable. Like other cases, variation in property values does not change the overall stability of the solutions.

5. Summary and discussion

We investigate the linear stability of a mathematical model of gas transport from an encapsulated bubble which explicitly

Table 2
Stability of solutions 4–6.

Equilibrium solution	f	E^s (N/m)	$\widehat{R}_{eqb}$	λ_1	λ_2
4	1.5	0.04	1.1249	-3.7×10^{-6}	-3.64×10^{-4}
5	1.4	0.01	1.5893	-2.62×10^{-6}	-3.57×10^{-5}
6	1.4	0.01	0.9438	6.38×10^{-5}	-4.43×10^{-6}

accounts for hindered permeability through the encapsulation and encapsulation elasticity. We consider an air bubble as well as bubbles which contain air and a second gas. The equation predicts several equilibriums for different conditions. When we impose non-negativity on effective surface tension (consisting of reference surface tension and the elastic stress in the encapsulation) bubbles can only be stable in case of saturated or oversaturated liquid. An inelastic encapsulation leads to neutral stability when surface tension is zero. An elastic encapsulation can stabilize the bubble against dissolution driven by surface tension. However, in an air-saturated medium, it can only reach a neutrally stable radius. At this radius the effective surface tension is zero, and as the radius is further reduced, it still remains zero, and therefore reaches a new equilibrium. One notes that this could lead to a continual decrease of the radius by fluctuation. On the other hand, treating the encapsulation elasticity to be an independent property and allowing the encapsulation to experience a net compressive stress (negative effective surface tension) achieves a stable radius. We provide physical mechanisms underlying the stability or instability of different equilibrium radii. The stability of the solutions is not affected by the second gas, in that one of the eigenvalues retains the same sign as that of the air bubble case. We find that the second eigenvalue depends on the properties of the second gas. Both eigenvalues vary with radius of the bubble. The linear stability results are in conformity with previous numerical solution.

Acknowledgments

K.S. acknowledges support from NSF CBET-0651912 and NIH P20RR016472. This work is also partially supported by US Army Medical Research Material Command under W81XWH-08-1-0503, AHA Grant No. 06554414 and NIH HL081892.

Appendix A

The Jacobian obtained for linear stability analysis and for the positive perturbations ($\gamma > 0$) is comprised of following four elements.

$$\underline{\underline{J}}(1,1) = \frac{3\{9\widehat{R}^2 + 4\widehat{\gamma}_0\widehat{R} + 4\widehat{E^s}\widehat{R}(2\widehat{R}^2 - 1)\}}{(3\widehat{R}^3 + 2\widehat{\gamma}\widehat{R}^2 + 2\widehat{E^s}\widehat{R}^4)^2}\left[\frac{\beta L_A(A - f\widehat{R}^3)}{(\alpha_A + \widehat{R})} + \frac{L_F\{\widehat{R}^3 + \widehat{\gamma}\widehat{R}^2 - A\}}{(\alpha_F + \widehat{R})}\right] - \frac{3}{(3\widehat{R}^3 + 2\widehat{\gamma}\widehat{R}^2 + 2\widehat{E^s}\widehat{R}^4)} \times \left[\frac{-3\beta L_A f\widehat{R}^2}{(\alpha_A + \widehat{R})} + \frac{\beta L_A(A - f\widehat{R}^3)}{(\alpha_A + \widehat{R})(\alpha_F + \widehat{R})} + \frac{L_F(3\widehat{R}^2 + 2\widehat{\gamma}\widehat{R} + 2\widehat{E^s}\widehat{R}^4)}{(\alpha_F + \widehat{R})} + \frac{L_F\{\widehat{R}^3 + \widehat{\gamma}\widehat{R}^2 - A\}}{(\alpha_F + \widehat{R})(\alpha_A + \widehat{R})}\right] + \frac{3}{(3\widehat{R}^3\widehat{\gamma}\widehat{R}^2 + 2\widehat{E^s}\widehat{R}^4)}\left[\frac{\beta L_A(A - f\widehat{R}^3)}{(\alpha_A + \widehat{R})} + \frac{L_F\{\widehat{R}^3 + \widehat{\gamma}\widehat{R}^2 - A\}}{(\alpha_F + \widehat{R})}\right]\left[\frac{\alpha_A + \alpha_F + 2\widehat{R}}{(\alpha_F + \widehat{R})(\alpha_A + \widehat{R})}\right]$$

$$\underline{\underline{J}}(1,2) = \frac{-3}{(3\widehat{R}^3 + 2\widehat{\gamma}\widehat{R}^2 + 2\widehat{E^s}\widehat{R}^4)}\left[\frac{\beta L_A}{(\alpha_A + \widehat{R})} - \frac{L_F}{(\alpha_F + \widehat{R})}\right]$$

$$\underline{\underline{J}}(2,1) = 3\beta L_A\left[\frac{3f\widehat{R}^3(\alpha_A + \widehat{R}) + (A - f\widehat{R}^3)(\alpha_A + \widehat{R}) + (A - f\widehat{R}^3)\widehat{R}}{(\alpha_A + \widehat{R})^2\widehat{R}^2}\right]$$

$$\underline{\underline{J}}(2,2) = -\frac{3\beta L_A}{(\alpha_A + \widehat{R})\widehat{R}}$$

For negative perturbations ($\gamma = 0$), the elements of first row of the Jacobian get changed as the transient equation for bubble radius takes the different form.

$$\underline{\underline{J}}(1,1) = \frac{3\{6\widehat{R} + 8\widehat{E^s}\widehat{R}^3\}}{(3\widehat{R}^3 + 2\widehat{E^s}\widehat{R}^4)^2}\left[\frac{\beta L_A(A - f\widehat{R}^3)}{(\alpha_A + \widehat{R})} + \frac{L_F(\widehat{R}^3 - A)}{(\alpha_F + \widehat{R})}\right] - \frac{3}{(3\widehat{R}^3 + 2\widehat{E^s}\widehat{R}^4)}\left[\frac{-3\beta L_A f\widehat{R}^2}{(\alpha_A + \widehat{R})} + \frac{\beta L_A(A - f\widehat{R}^3)}{(\alpha_A + \widehat{R})(\alpha_F + \widehat{R})} + \frac{3L_F\widehat{R}^2}{(\alpha_F + \widehat{R})} + \frac{L_F\{\widehat{R}^3 - A\}}{(\alpha_F + \widehat{R})(\alpha_A + \widehat{R})}\right] + \frac{3}{(3\widehat{R}^3 + 2\widehat{E^s}\widehat{R}^4)} \times \left[\frac{\beta L_A(A - f\widehat{R}^3)}{(\alpha_A + \widehat{R})} + \frac{L_F(\widehat{R}^3 - A)}{(\alpha_F + \widehat{R})}\right]\left[\frac{\alpha_A + \alpha_F + 2\widehat{R}}{(\alpha_F + \widehat{R})(\alpha_A + \widehat{R})}\right]$$

$$\underline{\underline{J}}(1,2) = \frac{-3}{(3\widehat{R}^3 + 2\widehat{E^s}\widehat{R}^4)}\left[\frac{\beta L_A}{(\alpha_A + \widehat{R})} - \frac{L_F}{(\alpha_F + \widehat{R})}\right].$$

References

[1] R.E.A. Arndt, Annual Review of Fluid Mechanics 13 (1981) 273–328.
[2] R.E.A. Arndt, R.L. Voigt, J.P. Sinclair, P. Rodrique, A. Ferreira, Journal of Hydraulic Engineering – ASCE 115 (1989) 1297–1315.
[3] L. d'Agostino, L. Torre, A. Pasini, A. Cervone, Journal of Fluids Engineering – Transactions of the ASME 130 (2008).
[4] F.C. Rubio, A.S. Miron, M.C.C. Garcia, F.G. Camacho, E.M. Grima, Y. Chisti, Chemical Engineering Science 59 (2004) 4369–4376.
[5] R.V. Shohet, S.Y. Chen, Y.T. Zhou, Z.W. Wang, R.S. Meidell, T.H. Unger, P.A. Grayburn, Circulation 101 (2000) 2554–2556.
[6] R.J. Price, D.M. Skyba, T.C. Skalak, S. Kaul, Circulation 98 (1998) 1264–1267.
[7] K. Ferrara, R. Pollard, M. Borden, Annual Review of Biomedical Engineering 9 (2007) 415–447.
[8] N. deJong, F.J. Tencate, C.T. Lancee, J.R.T.C. Roelandt, N. Bom, Ultrasonics 29 (1991) 324–330.
[9] K. Sarkar, A. Katiyar, P. Jain, Ultrasound in Medicine and Biology 35 (2009) 1385–1396.
[10] P.S. Epstein, M.S. Plesset, Journal of Chemical Physics 18 (1950) 1505–1509.
[11] D. Chatterjee, K. Sarkar, Ultrasound in Medicine and Biology 29 (2003) 1749–1757.
[12] D. Chatterjee, K. Sarkar, P. Jain, N.E. Schreppler, Ultrasound in Medicine and Biology 31 (2005) 781–786.
[13] K. Sarkar, W.T. Shi, D. Chatterjee, F. Forsberg, Journal of the Acoustical Society of America 118 (2005) 539–550.
[14] A. Katiyar, K. Sarkar, P. Jain, Journal of Colloid and Interface Science 336 (2009) 519–525.
[15] A. Kabalnov, J. Bradley, S. Flaim, D. Klein, T. Pelura, B. Peters, S. Otto, J. Reynolds, E. Schutt, J. Weers, Ultrasound in Medicine and Biology 24 (1998) 751–760.
[16] A. Kabalnov, D. Klein, T. Pelura, E. Schutt, J. Weers, Ultrasound in Medicine and Biology 24 (1998) 739–749.
[17] P.B. Duncan, D. Needham, Langmuir 20 (2004) 2567–2578.
[18] P.B. Duncan, D. Needham, Langmuir 22 (2006) 4190–4197.
[19] M.A. Borden, M.L. Longo, Langmuir 18 (2002) 9225–9233.
[20] W. Kloek, T. van Vliet, M. Meinders, Journal of Colloid and Interface Science 237 (2001) 158–166.
[21] M. Blank, Federation Proceedings 21 (1962) 151.
[22] M. Blank, V.K. La Mer, in: V.K. La Mer (Ed.), Retardation of Evaporation by Monolayers, Academic Press, New York, 1962, pp. 59–66.
[23] E. Lac, D. Barthes-Biesel, N.A. Pelekasis, J. Tsamopoulos, Journal of Fluid Mechanics 516 (2004) 303–334.